JOURNAL OF MATERIALS SCIENCE 24 (1989) 3319–3327

The deformation of oriented high density polyethylene

Part 2 *The formation of long crystalline fibrils at elevated temperatures*

JEAN M. BRADY*, EDWIN L. THOMAS
Department of Polymer Science and Engineering, University of Massachusetts, Amherst, Massachusetts 01003, USA

Thin, single crystal-like textured films of HDPE were uniaxially elongated at 56, 93 and 129° C along the chain direction. In all cases, the initial shish-kebab morphology was transformed via ⟨0 0 1⟩ crystal shear, chain slip and "defect" generation within the crystalline phase. Shear between shish-kebabs was observed at all temperatures and was identified by a rotation of lamellar normals away from the elongation direction. Craze-like structures developed at all temperatures as well, but only propagated laterally at temperatures above the alpha transition temperature of polyethylene. The evolution of the crystalline phase during deformation was imaged in detail by darkfield TEM. The generation of long (3 μm), thin crystalline fibrils ("protofibrils") of about 7 nm diameter indicated that the material had undergone strain-induced crystallization. Lateral connections between the original kebabs were retained during drawing in many cases, and constituted tie fibrils between adjacent "craze" fibrils. The processes which occurred in thin films at temperatures above the alpha transition and which gave rise to long crystals provided insight into the generation of a continuous crystalline phase in bulk polyethylene.

1. Introduction

In Part 1 of this work the room temperature deformation of oriented shish-kebab films of HDPE was investigated by transmission electron microscopy (TEM) [1]. This enabled the conversion of an initial shish-kebab–stacked lamellar morphology to a more chain extended fibrillar morphology to be viewed. This study analysed the influence of temperature on deformation processes and resultant morphology.

The deformation of polyethylene can be considered to be a flow process in which entanglements and crystallites serve as constraints to chain motion. Differences in deformation morphology as a function of deformation temperature can be interpreted in terms of the increase in chain mobility and crystalline phase ductility with increasing temperature. High temperatures reduce the yield stress of the crystalline phase, and cause it to deform in a visco-elastic manner. This is in contrast to deformation at lower temperatures where crystals behave more like rigid bodies until very high stresses are reached. The temperature at which PE crystals change from rigid bodies (which efficiently transfer stress) to ones which alleviate stress through flow processes when subjected to a cyclic low amplitude strain (less than 1%), is known as the alpha transition. The mechanisms associated with the alpha loss are believed to involve shear between and within mosaic blocks [2–4]. Such processes were evident in Part 1 [1].

Analogies were drawn between the deformation mechanisms and morphologies observed here for thin films and those found for bulk ultrahigh modulus polyethylene [5]. Highly drawn bulk polyethylene can exhibit a tensile modulus of up to 220 GPa and crystallinities exceeding 90% [6]. This modulus is of the same order of magnitude as the theoretical crystalline modulus of polyethylene (along the chain direction, room temperature), estimated to be 235 to 340 GPa [7, 8]. The attainment of such a high modulus in polyethylene suggests the presence of a sample-spanning (continuous) crystalline phase. The formation of such a continuous crystalline phase in ultrahigh modulus PE has been attributed to extensive strain-induced crystallization [5, 6, 9–11].

Strain-induced crystallization in polymers has been a topic of research for many years [12–17]. In polyethylene, strain-induced crystallization is known to occur at room temperature [18, 19]. At this temperature, however, the mobility of non-crystalline chains is constrained by both entanglements and crystals, much as crosslinks constrain chain motion in a crosslinked rubber. The application of stress perturbs the equilibrium distribution of chain conformations, making it possible to achieve low energy (trans) conformations. This results in chain orientation and extension. When a sufficient number of chains laterally align, a stable chain-extended crystal nucleus forms and further

Present address: Mobil Chemical Company, Research and Development, PO Box 240, Edison, New Jersey 08818-0240, USA.

0022–2461/89 $03.00 + .12

crystal growth ensues. If molecules disengage from crystals or disentangle and undergo chain relaxation, however, they will not strain crystallize. The propensity of a material to undergo strain-induced crystallization, and the resultant crystal perfection varies with the number density of entanglements, crosslinks, branches, or other hindrances to the crystallization process which constitute defects in the crystal lattice.

2. Experimental details

After preparing thin film samples as outlined in Part 1 [1], the deformation stage and sample were inserted into an air oven, and allowed at least 15 min to reach oven temperature. The films were deformed at three separate temperatures: 56, 93, and 129 (± 2)° C. The lower two temperatures were chosen to bracket the alpha transition temperature (about 73° at 1 h), whereas the highest temperature studies corresponded to deformation at the initial stages of melting. The films were elongated as described in Part 1 at a rate of 5×10^{-4} mm sec^{-1}. When the deformation was complete, the materials were allowed to cool for 1 h, were carbon coated and were then viewed by TEM (all while still strained in the stage). Care was employed while handling as-drawn films so as to avoid accidental room temperature deformation.

To better understand the high temperature deformation of as-drawn films, these materials were directly viewed by TEM using an electron microscope stage set at 122° C (purchased from GATAN of Warrendale, Pennsylvania). Due to heating of the stage and sample by the electron beam, it was difficult to attain the exact temperature of interest (129° C).

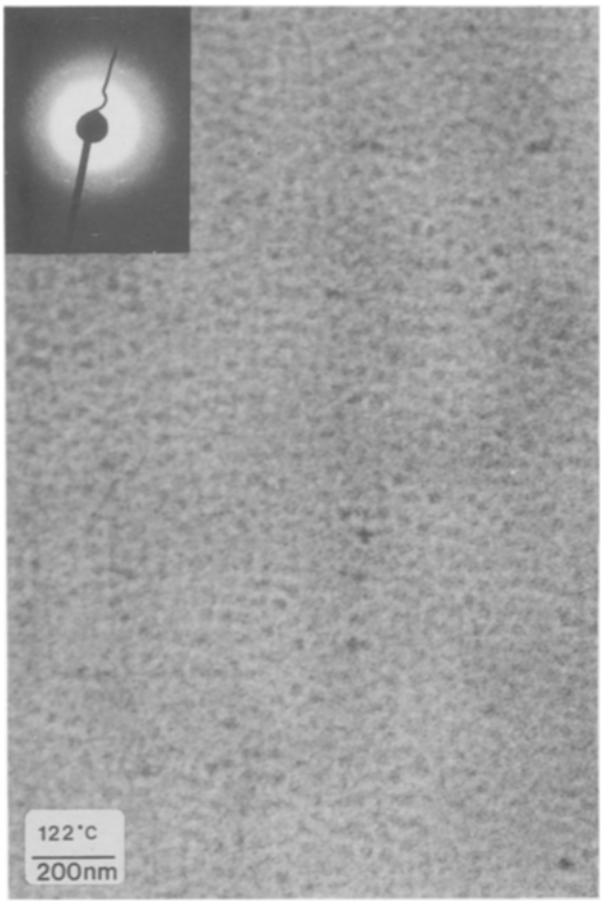

Figure 1 Brightfield micrograph of thin oriented HDPE film, taken at 122° C using a hot stage. Chain axis vertical in this and all subsequent micrographs.

3. Results

3.1. Undeformed film morphology at elevated temperatures

The main microstructural feature observed at 122° C was that the films had lost their lamellar character (Fig. 1). In addition, electron diffraction patterns displayed a prominent amorphous halo, indicating that a significant amount of thermally induced melting had occurred. The diffraction pattern of HDPE at 122° C (Fig. 1, inset) had only one faint equatorial reflection, which appeared to arise from the merger of the (1 1 0) and (2 0 0) reflections.

3.2. Deformation microstructure

The microstructures which evolved upon deformation at elevated temperatures will now be compared with those seen in films deformed at room temperature [1]. The initial observable stages of deformation at elevated temperatures involved cavitation of the non-crystalline phase (Fig. 2), equivalent to that seen for room temperature deformation. The films appeared similar to deformed hard elastic fibres [20–22]. Further elongation at 93 and 129° C fostered cavitation, microfibrillation and eventually the lateral growth of craze-like regions, henceforth referred to as crazes (Fig. 3). This degree of deformation was necessarily accompanied by some plastic deformation of shish-kebabs. This was in contrast to what was seen when films were

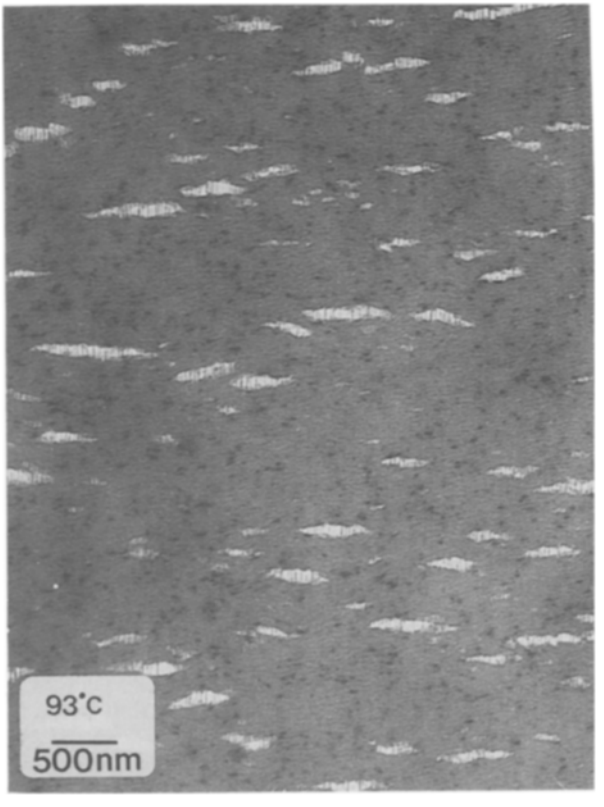

Figure 2 Brightfield micrograph of HDPE elongated parallel to the chain axis at 93° C showing the early stages of craze formation.

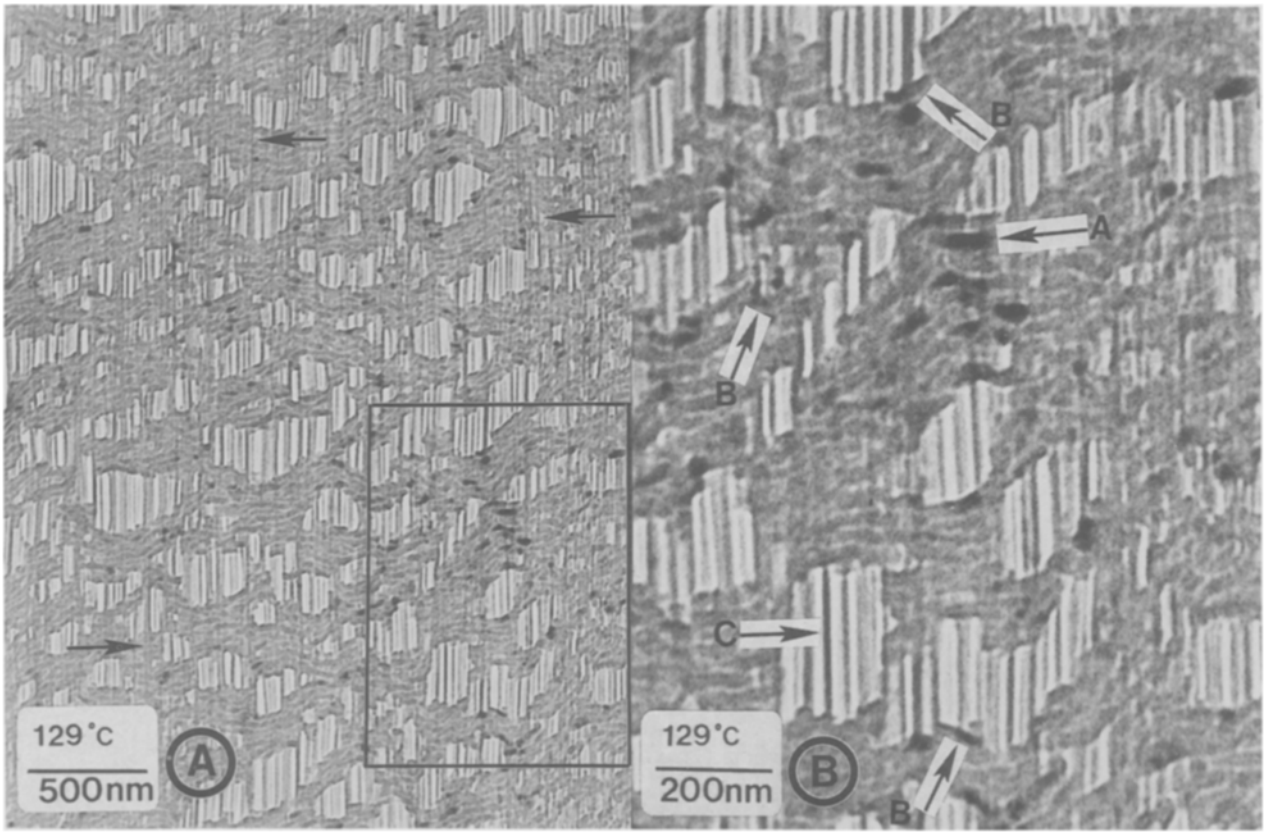

Figure 3 Brightfield micrograph of HDPE elongated parallel to the chain axis at 129° C revealing craze microstructure and shish-kebabs being drawn into microfibrils at (a) low magnification showing how shish-kebabs are drawn into microfibrils (arrows) and (b) high magnification showing relatively undeformed lamellae (A), lamellae being surface drawn into microfibrils (B) and strain-induced crystallization in microfibrils (C).

deformed along the chain direction at 25 and 56° C, where shish crystals apparently arrested such lateral craze growth.

Films elongated at 93 and 129° C deformed very non-uniformly. Microfibrillated (crazed) regions were highly strained while the rest of the film appeared essentially unaltered. Indeed, relatively undeformed crystals were seen diffracting in Fig. 3b in lamellar stacks (region A) whereas deformed crystallites could be seen at the craze interface as they were drawn into microfibrils (regions B). In some microfibrils (craze fibrils), the strain was high enough to bring about strain-induced crystallization (Fig. 3b, region C) similar to that seen previously [23]. It is probable that some yielding occurred in lamellar regions, but to a much lesser extent than in crazed regions. An idealized version of crazing in semicrystalline polymers based on these TEM observations is shown schematically in Fig. 4. This closely resembled the depiction of crazing set forth by Friedrich [24] except numerous craze fibrils strain crystallized and were laterally interconnected in the present case.

Microfibril diameters (10 nm) and lateral separation distances (about 15 to 30 nm) were essentially the same as those of shish-kebabs in the undeformed film. This suggested that each microfibril arose from an individual shish-kebab. This was verified by the observation that shish-kebabs in lamellar regions fed directly into microfibrils (Fig. 3a, arrows). This same observation concerning shish and craze fibril diameters was made for gel-spun fibres of ultrahigh molecular weight polyethylene (UHMWPE) [25]. At high stresses, the original shish-kebabs were transformed into a more chain-extended form, in which the average kebab thickness was reduced from about 30 to 7 nm (Fig. 5) and the extended chain shish core appeared more prominent. As this latter size borders on the resolution limits of the diffraction contrast darkfield imaging technique used, the kebabs were often difficult to detect. In fact, the elongated shish-kebabs were eventually transformed into crystalline fibrils of essentially uniform diameter. Such long, thin, needle-like crystalline microfibrils will be henceforth called protofibrils. They are believed to constitute the fundamental structural element in ultradrawn polyethylene.

In many cases, protofibrils appeared by darkfield TEM to diffract uniformly along their entire length. In other cases, however, protofibrils appeared to be comprised of a series arrangement of very small simultaneously diffracting crystalline blocks. Such a morphology was previously seen in ultradrawn bulk PE [5]. The simultaneous diffraction of these blocks suggested that they were interconnected by (unresolvable) crystalline bridges which could have formed by strain-induced crystallization. The generation of similar (very small) blocks during room temperature deformation of thin films implied that they were remnants of the original chain-folded kebabs, organized into a fibrillar structure.

Microfibrils formed by means of the decrystallization and elongation of shish-kebabs. The decrystallization process was shown schematically in Part 1 [1]. The studies made at elevated temperatures provide further support of the deformation mechanisms outlined in

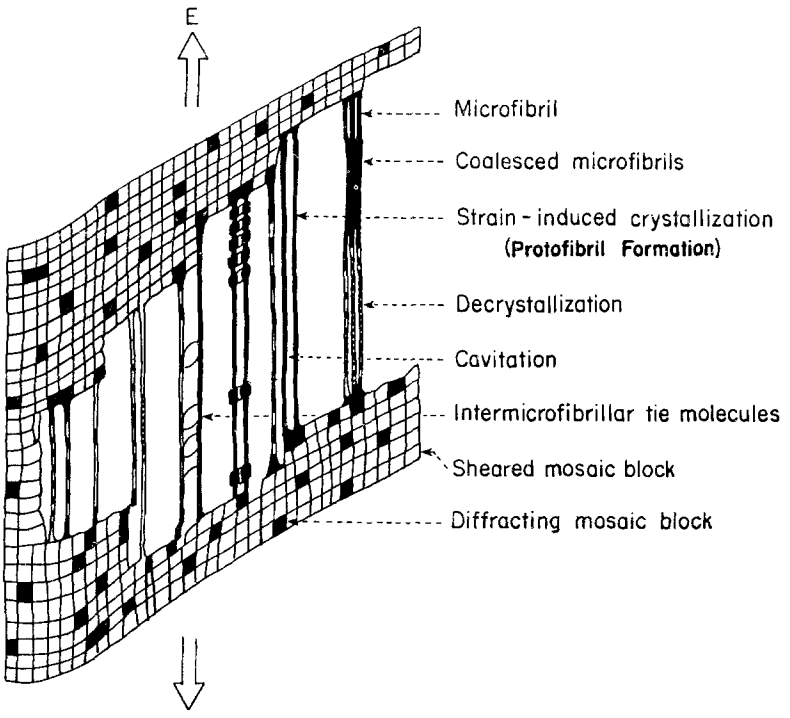

Figure 4 Idealized schematic of HDPE elongated parallel to the chain axis at 129° C. For simplicity, the amorphous phase was depicted by dark lines between mosaic blocks. Elongation direction (E) as indicated. Microfibrils: 10 nm wide, 15 to 30 nm apart, 3 μm long crystals, oriented along elongation direction.

Part 1. Darkfield micrographs complemented the brightfield micrographs shown in Part 1, providing the most detailed information yet on the decrystallization and drawing of kebabs into shish crystals (Figs 5 to 8). The early stages of crystalline phase deformation involved $\langle 0\,0\,1 \rangle$ crystal shear from the main kebab block (Figs 6, 7, regions A). Occasionally, the kebab became diamond-shaped (Fig. 6, region E and Fig. 8, inset). This was followed by additional shear until the kebab was transformed into a number of very narrow crystal remnants, positioned sequentially one after

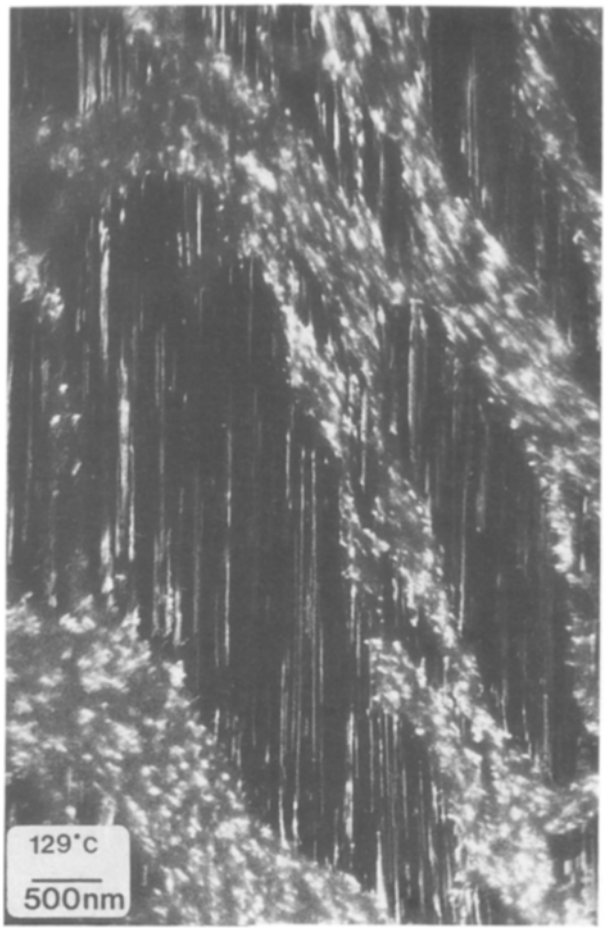

Figure 5 Darkfield micrograph of HDPE elongated parallel to the chain axis at 129° C showing extensive strain-induced crystallization in crazed regions.

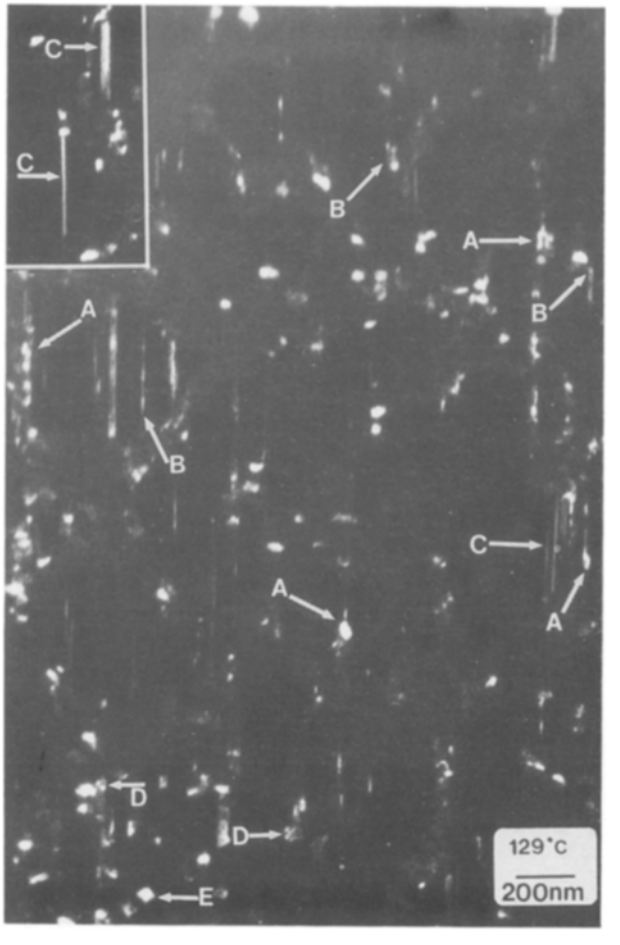

Figure 6 Darkfield micrograph of HDPE elongated parallel to the chain axis at 129° C showing crystal shear (A), more extensive shear (B), protofibrils (C), defects within crystals (D) and diamond-shaped crystallites (E).

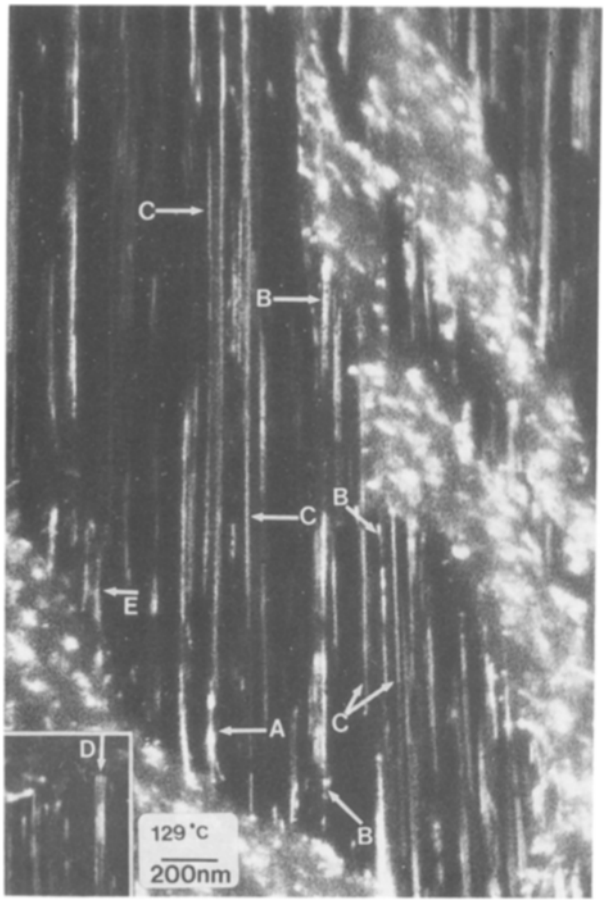

Figure 7 Higher magnification of Fig. 5. Darkfield micrograph of HDPE elongated parallel to the chain axis at 129° C showing crystal shear (A), more extensive shear (B), protofibrils (C), microfibrils which have laterally coalesced (D) and laterally interconnected microfibrils (E).

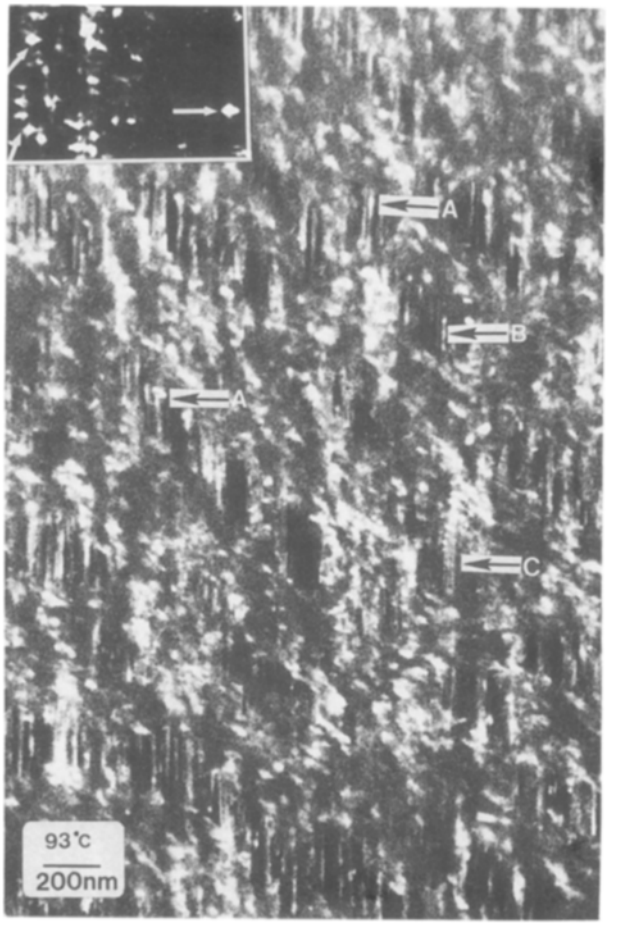

Figure 8 Darkfield micrograph of HDPE elongated parallel to the chain axis at 93° C showing crazes and diamond-shaped kebabs (inset).

another along the draw direction (Figs 6, 7 and 8, regions B), giving the appearance of a non-periodic alternation of crystalline and amorphous phases along the microfibril. Chain-folded kebabs were transformed into mosaic blocks of reduced crystal thickness (along the chain direction) by the generation of "defects" within crystals (Fig. 6, regions D). Crystallization subsequently occurred where the non-crystalline phase had become extended and aligned. The final result was the formation of photofibrils within crazes (Figs 6, 7 and 8, regions C). The fact that lamellar regions, which were much less strained than crazed ones, did not contain long crystals indicated that protofibril formation involved strain-induced crystallization. In some cases, microfibrils laterally coalesced (Fig. 7, region D), while in other cases they appeared to be laterally interconnected by tie fibrils (Fig. 7, region E). In brightfield micrographs, protofibrils appeared as faint striations (Fig. 9). Darkfield and brightfield micrographs indicated that crystals up to 3 μm long were present in microfibrillated regions (Fig. 7, regions C). The reader is again referred to Fig. 4 for a summary of the microfibrillar structure.

During craze growth, lateral stresses (perpendicular to the chain axis) were relieved by cavitation between microfibrils, while longitudinal stresses (parallel to the chain axis) were relieved by shish-kebab elongation. The non-uniform extension of shish-kebabs in cavitated regions resulted in a significant amount of shear between neighbouring shish-kebabs in lamellar regions. This was detected by the rotation of lamellar normals away from the elongation direction (Fig. 3). This resulted in a cavity interface which formed an angle ranging from about 30° to 90° with the elongation direction (Fig. 9b). Lamellae laid along the cavity interface while shish-kebabs retained their initial orientation, the chain axis remaining parallel to the elongation direction. Shish-kebabs constituted lateral borders between crazed and lamellar material, apparently blunting stress concentrations at craze tips (Figs 3 and 9).

The deformation of HDPE at 93° C paralleled that at 129° C (Fig. 8). In both cases the material microfibrillated and formed long crystalline regions. It is believed that the major difference in deformation at these two temperatures involved the level of draw stress during microfibrillation, the resultant deformation morphologies being quite similar.

Deformation at 56° C resembled that discussed in Part 1 [1]. Elongation along the chain direction occurred globally throughout the film, and the material fibrillated into shish-kebabs. However, there appeared to be significantly more shear and flow at this temperature as a whole than that found for room temperature deformation. The deformation microstructure took on a network-like appearance (Fig. 10). Individual crystal blocks were relatively undefined, and the interface

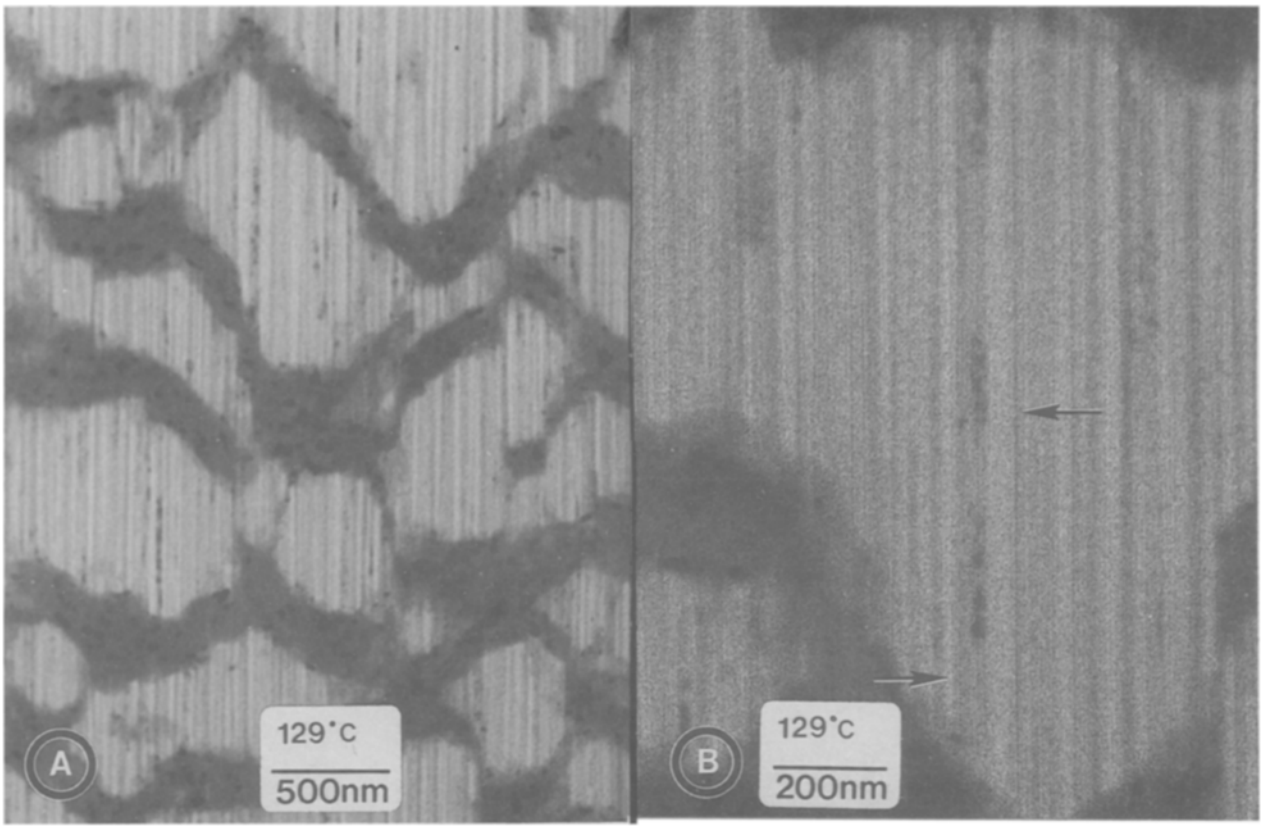

Figure 9 Brightfield micrograph of HDPE elongated parallel to the chain axis at 129° C showing craze microstructure and faint striations corresponding to protofibrils at (a) low magnification and (b) high magnification.

between highly deformed and slightly deformed material was quite diffuse. Each fibril in the network was of approximately constant diameter and contained crystal block remnants. The chain mobility at 56° C was apparently high enough to facilitate crystal shear, but not so high as to effect microfibrillation, significant strain-induced crystallization, protofibril formation, and the generation of extensive crystalline regions.

4. Discussion

4.1. Melting and decrystallization

In Part 1, the possibility of a rise in temperature and subsequent melting during decrystallization was ruled negligible, since the ambient temperature was 25° C (peak melting temperature of the PE being 135° C by differential scanning calorimetry), the elongation rate was low, and thin films were used. In the present experiments, however, the ambient temperature was (variously) higher, as was the possibility of partial melting before and/or during deformation. The microstructure of as-drawn (undeformed) HDPE film, viewed at 122° C, did in fact differ from that viewed at room temperature. A significant degree of (quiescent) melting had occurred at 122° C, resulting in a film composed of apparently isolated crystallites. Thus, the initial state of as-drawn films at 129° C prior to deformation was not lamellar. It is likely that the lateral cohesion between kebabs was poor due to surface melting [29], melting of small crystals [30] and a possible reduction in the number of tie molecules and entanglements interconnecting adjacent kebabs. This means that the lateral transfer of stress between shish-

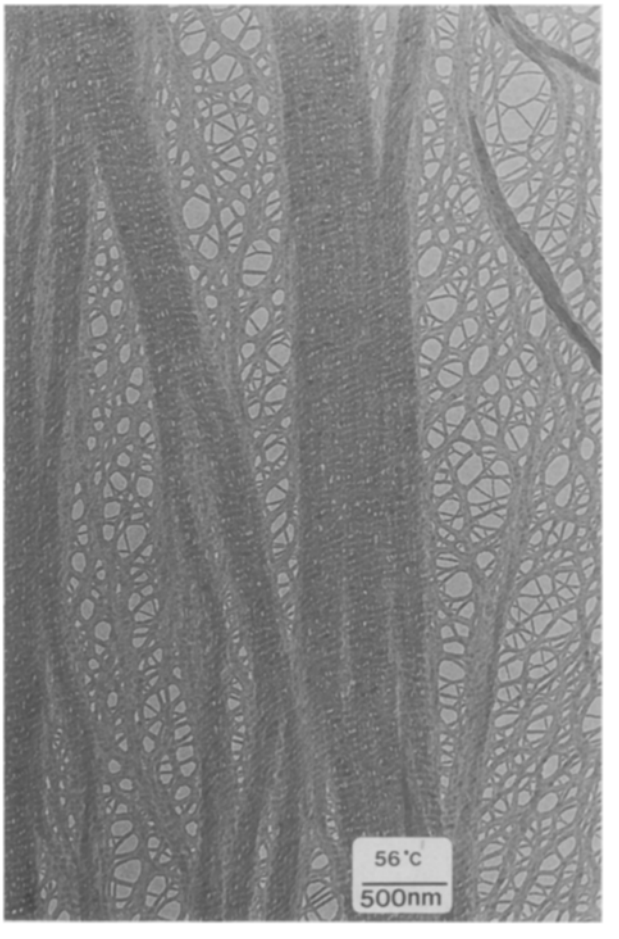

Figure 10 Brightfield micrograph of HDPE elongated parallel to the chain axis at 56° C showing fibrillation and network-like structure.

kebabs would be inefficient at high temperatures. Individual shish-kebabs would therefore easily fibrillate apart.

4.2. Electron microscopy as opposed to X-ray scattering techniques

The utility of TEM (especially using the darkfield mode) in detailing the transformation of morphology was clearly evident in the preceding micrographs. Indirect methods have previously been used to ascertain the presence of crystalline bridges between lamellae. For instance, wide angle X-ray scattering (WAXS) measurements have yielded a weight average crystal thickness (parallel to the chain direction) exceeding the average long period value obtained by small angle X-ray scattering (SAXS) [26]. Assuming uniform deformation throughout the sample, this implied that crystalline bridges had formed, spanning the amorphous layers of what was essentially a modification of the microfibrillar model of Peterlin [27]. However, the observations made here suggest that the continuous crystalline phase is comprised of long fibrillar crystals of essentially uniform diameter rather than a series arrangement of wide lamellae and narrow crystalline bridges. In fact, TEM observations indicated that the concept of uniform deformation is inappropriate for HDPE deformed at high temperatures. As shown in Fig. 4, HDPE elongated at 93 and 129° C deformed very non-uniformly along the elongation direction, high strains being achieved in crazed regions while the original lamellar morphology remained relatively intact in uncrazed regions. Since the microfibrils were non-periodic along the chain direction on the 10 to 50 nm length scale, only the (relatively undeformed) lamellar stacks would give rise to SAXS long period peaks. SAXS long period measurements would thus indicate an erroneously low degree of deformation. In contrast, both microfibrils and lamellae would contribute to WAXS crystal thickness measurements. Protofibrils in particular would give rise to a large average crystal thickness determination by WAXS. Thus, the utility of direct observation by microscopy (especially for heterogeneous systems), rather than scattering techniques, is underscored.

The studies made here paralleled another study in which bulk gel-spun fibres of UHMWPE were deformed and characterized by SAXS, WAXS and scanning electron microscopy (SEM) [28]. Many details of the deformation process could not be determined in this previous study, however, since the samples were gold coated for SEM, and diffraction contrast (and darkfield imaging) could not be employed. Thus, the details of the lamella to fibril transformation could not be determined. The darkfield micrographs shown here, on the other hand, gave insight into the decrystallization process, and enabled the undisputable identification of protofibrils and long crystalline regions in highly deformed areas. The fact that Van Hutten *et al.* [28] detected the same overall microfibrillated morphology as seen here indicated that strong analogies can be drawn between deformation in the bulk and in thin films.

4.3. Variation of crystal thickness with deformation temperature

Certain small angle X-ray scattering studies have indicated that the long period of bulk-deformed HDPE reflects only the deformation temperature and not the crystallization conditions of the original undeformed material [32–34]. Reductions in long period were at first explained in terms of thermally induced melting (arising from frictional losses during deformation) and subsequent recrystallization [33, 35]. Further analysis suggested that melting was facilitated by a reduction in melting temperature due to the presence of a negative lateral pressure during tensile deformation [34].

The dependence of crystal thickness and long period on deformation temperature can be explained in terms of decrystallization and strain-induced crystallization processes. The relative amounts of decrystallization and recrystallization which occur during deformation are temperature dependent. A reduction in the average crystal thickness following room temperature deformation can be explained in terms of "defect" generation within mosaic blocks, and the absence of significant strain-induced crystallization and annealing. The change in SAXS long period would depend on the extent of deformation (and non-crystallization phase elongation), and the degree of periodicity in deformed lamellar stacks. At high temperatures, both decrystallization and strain-induced crystallization as well as annealing occur. SAXS long period measurements (dominated largely by the relatively undeformed lamellar stacks) would indicate an increase in average long period due to the thermally induced melting of small crystals [30] as well as amorphous phase elongation. An increase in average crystal thickness would result from annealing as well as decrystallization followed by strain-induced crystallization in crazed regions. Therefore, deformation at high temperatures would result in an increase in crystal thickness and long period, while deformation at low temperature would result in a decrease in crystal thickness and possibly long period, in agreement with the previously cited SAXS and WAXS data. It is not necessary to invoke a deformation-induced temperature rise and global melting and recrystallization to explain SAXS and WAXS observations. It is proposed that the "negative lateral pressure" mechanism of crystal destruction propounded by Peterlin [34] and earlier by Hookway [36], parallels the decrystallization processes which were shown here.

4.4. Craze growth

Craze growth involved substantial plastic deformation. Kebabs sheared apart and fed into shish crystals in a localized zone at the craze interface. In glassy polymers, this process is termed surface drawing. It results in a variation of draw ratio throughout the resultant craze, the tip and "midrib" regions of the craze experiencing the least amount of surface drawing and, therefore, displaying the highest draw ratio [31]. In the present study, no such draw ratio variations, as revealed by the preferential formation of long crystals in a given region of the craze, were detected. This suggested that

an analogous "midrib" region of high strain was not present in PE.

While microfibrils elongated via decrystallization and surface drawing at craze interfaces, kebab remnants already within the interiors of the cavities underwent further shear (Figs 5 and 7). In this way, microfibrils elongated both by surface drawing, in which new material is fed into the craze, and draw-down, in which material already within the craze is further deformed. The degree of microfibril draw-down accessed here was insufficient to cause microfibril fracture. The draw ratio of microfibrils was, however, increased. The resultant high degree of chain extension and alignment gave rise to strain-induced crystallization and protofibril formation.

At low deformation temperatures (25 and 56° C), crazes nucleated but did not propagate perpendicular to the chain direction, due to the higher yield stress and greater reinforcing capabilities of the crystalline phase. Instead, cavities coalesced between shish-kebabs and resulted in heterogeneous fibrillation. Although the relatively high stress levels in fibrils resulted in some decrystallization, the resultant strain and chain alignment was not sufficient to bring about appreciable strain-induced crystallization at these lower temperatures.

4.5. Continuous crystal formation

The studies done here on thin films constitute only one approach towards understanding structure–property relationships in PE. Previous work entailed a darkfield TEM investigation of solid state extruded–post drawn (SSE–PD) polyethylene which had been drawn to various degrees, the ultradrawn material having a tensile modulus exceeding 175 GPa [5]. By studying the deformation behaviour of thin films, the processes giving rise to an ultrahigh modulus in PE could be better understood. Specifically, darkfield microscopy of thin films allowed the details of the decrystallization and (re)crystallization processes which appeared to accompany SSE–PD to be observed. Indeed, TEM micrographs of thin films revealed the much greater ductility of the crystalline phase and the associated increase in strain-induced crystallization at temperatures above the alpha transition temperature.

A comparison of the microstructures observed for thin films with those of the ultrahigh modulus SSE–PD bulk samples revealed similar deformation morphologies [5]. In both cases, the highly drawn materials were very crystalline and were comprised of long (up to 3 μm) fibrillar crystalline regions. Protofibrils of equivalent structure formed by both processes. Moreover, microfibrils laterally coalesced in the thin films much as protofibrils did in SSE–PD material. This supported a continuous crystalline phase model comprised of laterally coalesced protofibrils [5]. The well known increase in tensile modulus with draw can thus be attributed to an increase in non-crystalline phase extension and extensive strain-induced crystallization.

5. Conclusions

Darkfield mode TEM provided a window through which the details of the conversion of chain-folded to chain-extended crystals and the processes leading to crystalline phase continuity could be seen. The advantages of directly imaging the deformation morphology as opposed to obtaining indirect (averaged) X-ray scattering data was illustrated. Observation by TEM indicated that neither of the two extreme continuous crystalline phase models: microfibrils containing periodically alternating chain-folded lamellae and amorphous phases, with chain-extended crystalline bridges spanning the amorphous phase; nor an extensive chain-extended crystal containing defects, were accurate representations of the microstructure of polyethylene drawn from thin, highly oriented, single crystal-like textured, shish-kebab morphology films. Instead, the crystalline phase consisted of lamellae and protofibrils, the formation and structure of which is summarized in the following.

At low temperatures (25 and 56° C) the thin, oriented HDPE films elongated uniformly along the chain orientation direction, whereas non-uniform elongation was found at high temperatures (93 and 129° C). In the latter case the HDPE film consisted of highly extended material in crazed regions and relatively undeformed lamellar stacks elsewhere. The crazing process involved the same decrystallization mechanisms as seen during room temperature deformation. Darkfield micrographs enabled the detailed visualization of $\langle 0\,0\,1 \rangle$ crystal shear and "defect" generation within crystals, as well as the final conversion of chain-folded crystals to much longer more chain-extended crystals. However, at temperatures above the alpha transition temperature, craze fibrils underwent strain-induced crystallization, forming long crystalline microfibrils, termed protofibrils, of almost uniform diameter (7 nm). Crystalline regions as long as 3 μm formed. A comparison of craze fibril microstructure with that obtained for ultradrawn (SSE–PD) fibres as well as elsewhere for bulk gel-drawn PE indicated that the morphology seen in these thin film studies is a good representation of that which forms in the bulk.

Such comparisons suggested that the tensile drawing of thin films at temperatures above the alpha transition can be used to better understand the formation of a continuous crystalline phase. Both thin films and SSE–PD PE deformed by the same decrystallization and stain-induced crystallization mechanisms, and led to an increase in crystallinity as well as the formation and lateral coalescence of protofibrils. Indeed, the structure of protofibrils seen in both cases was virtually identical. In addition to lateral coalescence, microfibrils in cavitated regions of thin films retained lateral interconnections by means of tie fibrils.

The main difference between deformation at high and low temperatures was attributed to the lower yield stress and enhanced chain mobility at high temperatures. Although partial thermally induced melting had occurred at 122° C, as indicated by viewing as-drawn films at this temperature, it was shown that even material which had not undergone significant melting (e.g. at 93° C), as determined by differential scanning calorimetry, formed crazes, which propagated perpendicular to the chain axis, as long as it was above the

alpha transition temperature (about 73° C). At lower temperatures (25 and 56° C), no such lateral crazes nor the associated long crystals were detected. The absence of crazes (for material elongated along the chain orientation direction) at temperatures below the alpha transition was attributed to the higher yield stress of the crystalline phase, craze propagation being arrested by shish crystals.

Acknowledgements

We would like to thank the Materials Research Laboratory, University of Massachusetts, for the use of their facilities, and gratefully acknowledge the support of the National Science Foundation, Grant No. DMR84-06079 (Polymers Program).

References

1. J. M. BRADY and E. L. THOMAS, *J. Mater. Sci.*
2. T. KAJIYAMA, T. OKADA, A. SAKODA and M. TAKAYANAGI, *J. Macromol. Sci., Phys.* **B7** (1973) 583.
3. M. TAKAYANAGI and T. KAJIYAMA, *ibid.* **B8** (1973) 1.
4. A. TANAKA, E. P. CHANG, B. DELF, I. KIMURA and R. S. STEIN, *J. Polym. Sci., Phys. Edn* **11** (1973) 1891.
5. J. M. BRADY and E. L. THOMAS, *Polymer* in press.
6. T. KANAMOTO, A. TSURUTA, K. TANAKA, M. TAKEDA and R. S. PORTER, *Polymer J.* **15** (1983) 327.
7. I. SAKURADA, T. ITO and K. NAKAMAI, *J. Polym. Sci., Phys.* **15** (1966) 75.
8. T. SHIMANOUCHI, M. ASAHINA and S. ENOMOTO, *J. Polym. Sci.* **59** (1962) 93.
9. A. PENNINGS and K. E. MEIHUIZEN, in "Ultra-High Modulus Polymers", edited by A. Ciferri and I. M. Ward (Applied Science Publishers, Essex, England, 1979) Chap. 3.
10. P. SMITH and P. J. LEMSTRA, *J. Mater. Sci.* **15** (1980) 505.
11. A. E. ZACHARIADES, W. T. MEAD and R. S. PORTER, *Chem. Rev.* **80** (1980) 351.
12. A. PETERLIN, *Polym. Eng. Sci.* **16** (1976) 126.
13. G. S. Y. YEH, *ibid.* **16** (1976) 145.
14. *Idem, ibid.* **16** (1976) 138.
15. T. NAGASAWA and Y. SHIMOMURA, *J. Polym. Sci., Phys. Edn.* **12** (1974) 2291.
16. A. PENNINGS, *J. Polym. Sci., Polym. Symp.* **59** (1977) 55.
17. E. H. ANDREWS, *Proc. R. Soc.* **A277** (1964) 562.
18. M. MILES, J. PETERMANN and H. GLEITER, *J. Macromol. Sci.* **B12** (1976) 523.
19. F. DECANDIA, V. VITTORIA and A. PETERLIN, *J. Polym. Sci., Phys.* **23** (1985) 1217.
20. B. S. SPRAGUE, *J. Macromol. Sci., Phys.* **B8** (1973) 157.
21. S. L. CANNON, G. B. McKENNA and W. O. STATTON, *J. Polym. Sci., Macromol. Rev.* **11D** (1976) 209.
22. B. CAYROL and J. PETERMANN, *J. Polym. Sci., Phys. Edn* **12** (1974) 2169.
23. R. M. GOHIL and J. PETERMANN, *ibid.* **17** (1979) 525.
24. K. FRIEDRICH, "Advances in Polymer Science, 52/53", edited by H. H. Kausch (Springer, New York, 1983) p. 225.
25. A. R. POSTEMA, W. HOOGSTEEN and A. J. PENNINGS, *Polym. Commun.* **28** (1987) 148.
26. A. G. GIBSON, G. R. DAVIES and I. M. WARD, *Polymer* **19** (1978) 683.
27. A. PETERLIN, *J. Mater. Sci.* **6** (1971) 490.
28. P. F. VAN HUTTEN, C. E. KONING and A. J. PENNINGS, *ibid.* **20** (1985) 1556.
29. Y. TANABE, G. R. STROBL and E. W. FISCHER, *Polymer* **27** (1986) 1147.
30. D. P. POPE and A. KELLER, *J. Polym. Sci., Phys. Edn.* **14** (1976) 821.
31. B. D. LAUTERWASSER and E. J. KRAMER, *Phil. Mag.* **A39** (1979) 469.
32. R. CORNELUISSEN and A. PETERLIN, *Makromolekulare Chemie* **105** (1967) 193.
33. A. PETERLIN and K. SAKAOKU, *J. Appl. Phys.* **38** (1967) 4152.
34. A. PETERLIN, in "Advances in Polymer Science and Engineering," edited by K. D. Pae, D. R. Morrow and Y. Chen (Plenum, New York, 1972) p. 1.
35. A. PETERLIN, *Kolloid Z. Z. Polymere* **216–217** (1967) 129.
36. D. C. HOOKWAY, Proceedings of the Textile Institute and Fiber Society Conference, Boston, Massachusetts, September 1957, p. 292.

Received 6 July
and accepted 18 November 1988